Application of Molecular Modeling to C−H Activation in Organoiron Compounds

K. Angermund,* S. Geier,† P. W. Jolly, M. Kessler, C. Krüger, and F. Lutz

Max-Planck-Institut für Kohlenforschung, D-45466 Mülheim an der Ruhr, Germany

Received December 17, 1997

Molecular modeling has been applied to the products of the reaction between bidentate-phosphine-stabilized iron species and 1,5-hexadiene. On the basis of the TRIPOS force field, a complete set of parameters for an iron atom in a tetrahedral environment has been derived and the accessible molecular surface (AMS) model has been used to estimate the effect of the bidentate ligand upon the free coordination surface for a variety of $(R_2P(CH_2)_nPR_2)Fe$ fragments. The results suggest that the course of the reaction is largely controlled by steric factors associated with the bidentate ligands: sterically demanding ligands lead to a small AMS at the metal atom, and further reaction of the coordinated hexadiene is hindered; less demanding ligands lead to a larger AMS, which enables the metal atom to interact with a methylenic H atom with resulting H transfer and formation of a $(\eta^5\text{-}1\text{-}MeC_5H_6)Fe-H$ species.

Introduction

In previous publications, we have suggested that the course of the reaction between bidentate-phosphine-stabilized iron species and a nonconjugated diene is controlled mainly by the steric requirements of the donor ligand. For example, the reaction with 1,5-hexadiene leads to the formation of the paramagnetic $(\eta^2{:}\eta^2\text{-}1,5\text{-}C_6H_{10})Fe^0$ species **1** (R = Pr^i, n = 3) in the presence of bis(diisopropylphosphino)propane and of the diamagnetic $(\eta^5\text{-}1\text{-}MeC_5H_6)Fe-H$ species **3** (R = Pr^i, n = 2) in the presence of bis(diisopropylphosphino)ethane without either compound showing a tendency to react further below the decomposition temperature. Compounds of type **1** are formed not only where R is isopropyl (Pr^i) but also where R is cyclopentyl (cyp) and n = 2 while compounds of type **3** are formed where R is isopropyl and n = 3−5 or where R is *tert*-butyl (Bu^t) and n = 2 as well as in the presence of triethylphosphine. A mixture of **1** and **3** is the product of the reaction where R is cyclohexyl (cyh) and n = 2.[1,2]

We assume that these reactions proceed as shown in Scheme 1. Initially an $(R_2P(CH_2)_nPR_2)Fe^0$-species is generated to which the 1,5-hexadiene coordinates in an $\eta^2{:}\eta^2$-manner. If the bidentate ligand is sterically demanding, then the reaction terminates at this point and **1** is isolated. In the presence of less demanding ligands, the metal atom presumably interacts with a methylenic C−H group of the diene in an agostic manner (**2**) and this is followed by C−H bond cleavage and hydrogen transfer to the metal to give **3**.

The extended Hückel MO calculations included in a previous publication[2] suggest that while electronic factors may well play a role in influencing the course of reaction where steric effects are relatively insignificant, they do not have a decisive effect where steric effects are more marked. Whereas Dreiding models are sufficient to demonstrate qualitatively that the $(Pr^i_2PC_2H_4PPr^i_2)Fe$ and $(Pr^i_2PC_3H_6PPr^i_2)Fe$ fragments do indeed have different space-filling properties, attempts to make allowance for conformational flexibility and to put these observations on a more quantitative basis require the application of molecular modeling and are the topics of this publication.

Although computer-aided molecular design (CAMD) has established itself as an invaluable tool for determining, among others, energetically favored molecular conformations, the application to organoiron species has been hampered by a lack of force field parameters for this metal in a tetrahedral environment. Our solution of this problem based on the TRIPOS force field[3] will be described initially.

Scheme 1

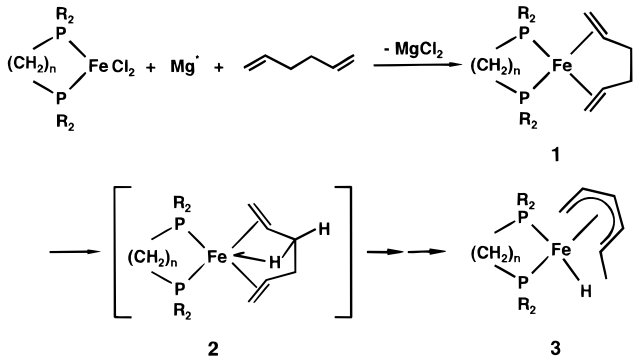

* To whom correspondence should be addressed.

† Part of the doctoral thesis submited to the Ruhr-Universität-Bochum in January 1996.

(1) Gabor, B.; Goddard, R.; Holle. S.; Jolly, P. W.; Krüger, C.; Mynott, R.; Wisniewski, W. *Z. Naturforsch.* **1995**, *50*B, 503.

(2) Geier, S.; Goddard, R.; Holle, S.; Jolly, P. W.; Krüger, C.; Lutz, F. *Organometallics* **1997**, *16*, 1612.

(3) (a) SYBYL 6.0 and 6.2; TRIPOS Associates, Inc., St. Louis, MO. (b) Clark, M.; Cramer, R. D., III; Van Opdenbosch, N. *J. Comput. Chem.* **1989,** *10*, 982.

S0276-7333(97)01110-2 CCC: $15.00
Publication on Web 05/19/1998

Table 1. Comparison of Structural Data for the X-ray Structures of 4−7 and the Equilibrium Values and Final Force Constants for the Corresponding Potential Functions

	bond length (Å) or valence angle (deg)					final force constant
param	**4a**	**5**	**6**	**7**	equilibrium value	(kcal mol^{-1} Å^{-2})
Fe.th−P.3	2.280	2.308	2.266	2.298	2.266	288
	2.290	2.313	2.266	2.321		
Fe.th−MpEt	1.949	1.981	1.977	1.946	1.968	340
	1.969	1.983	1.977	1.958		
P.3−Fe.th−P.3	95.0	99.26	106.3	92.9	109.5	0.005
P.3−Fe.th−MpEt	110.8	113.9	110.0	102.0	109.5	0.006
	113.5	115.0	110.0	107.6		
	115.1	119.8	110.0	112.0		
	118.2	120.1	110.0	113.2		
MpEt−Fe.th−MpEt	104.4	90.4	111.0	124.5	109.5	0.007

Force Field Parameters for Iron

We have already successfully extended TRIPOS force field parameters for Zr, Ni, Co, and Rh[4−8] and have used these successfully to model a number of catalytically relevant organometallic compounds. The procedure applied (empirical structure based paramerization) has been described in detail in previous publications[4a,b,5a] and is based upon the extraction of reference data such as bond lengths, bond angles, and the periodicity of the torsional potential from crystal structures of suitable compounds. In the case of iron, the paucity of data is problematic and limits the general application of the developed parameters: in contrast to the 18-electron (η^2:η^2-diene)Fe compounds containing *three* P-donor ligands, few 16-electron species containing only *two* P-donor ligands have been studied and the four examples which we have considered are shown as **4**−**7**.[1,9,10]

The inclusion of only that isomer of **4** in which the 1,5-hexadiene has a *transoid* arrangement (**4a**) allows us to check that the calculated force field parameters developed accurately describe the major isomer, **4b**, in which the diene has a cisoid arrangement.

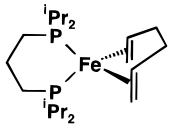

4a[1]

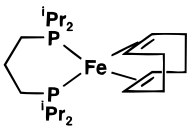

5[9]

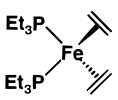

6[10]

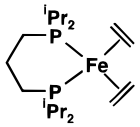

7[9]

We have previously demonstrated[4−8] that the so-called centroid topology (middle-point method), first introduced by Struchkov et al.,[11,12] can be successfully applied to describe the bonding of a metal-coordinated double bond in a force field. This model is shown schematically as **A** and **B**. The center of the coordinated double bond is occupied by a pseudoatom (Mp.Et) which is bonded to the metal atom and to the C atoms of the double bond (C.2m). The connectivity diagram is shown as **A** and a more realistic depiction of the geometry as **B**, in which the abbreviations (Fe.th = Fe atom in a tetrahedral environment, Mp.Et = middle point of the coordinated double bond (pseudoatom), C.2m = metal coordinates of an sp^2-hybridized C atom) correspond to the atom potential type description used in our extension to the TRIPOS force field. This model has been applied to the crystal structures of **4**−**7**. The experimentally determined values of selected bond lengths and valence angles at the iron center are summarized in Table 1. Since we were most interested in the dependence of the size of the accessible area at the metal center on the structure of the $R_2P(CH_2)_nPR_2$ ligands, an idealized tetrahedral coordination geometry at the iron atom was chosen. Together with relatively small force

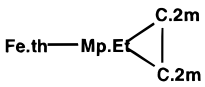

A

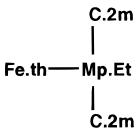

B

(4) (a) Nolte, M. Doctoral Dissertation, Universität Münster, 1992. (b) Angermund, K.; Hanuschik, A.; Nolte, M. Force Field Calculations on Zirconocene Compounds. In *Ziegler Catalysts*; Fink, G., Mülhaupt, R., Brintzinger, H. H., Eds.; Springer: Berlin, 1995. (c) Van der Leek, Y.; Angermund, K.; Reffke, M.; Kleinschmidt, R.; Goretzki, R.; Fink, G. *Chem. Eur. J.* **1997**, *3*, 585.

(5) (a) Lutz, F. Doctoral Dissertation, Universität Wuppertal, 1993. (b) Angermund, K.; Eckerle, A.; Lutz, F. *Z. Naturforsch.* **1995**, *50B*, 488.

(6) Krömer, R. Doctoral Dissertation, Universität Wuppertal, 1994.

(7) Kessler, M. Doctoral Dissertation, Universität Wuppertal, 1997.

(8) Bruckmann, J.; Krüger, C.; Lutz, F. *Z. Naturforsch.* **1995**, *50B*, 351.

(9) (a) Frings, A. J. Doctoral Dissertation, Universität Bochum, 1988. (b) Frings, A. J.; Jonas, K. Unpublished results. (c) **Single-crystal X-ray analysis of 5**:[9e] size, 0.54 × 0.40 × 0.36 mm; Enraf-Nonius CAD4 diffractometer; Mo Kα (graphite monochromator, λ = 0.710 69 Å), empirical formula, $C_{19}H_{42}P_2Fe{\cdot}0.5C_6H_{12}$; space group, $P2_1/n$; unit cell dimensions, a = 11.67(1) Å, b = 16.46(1) Å, c = 12.673(6) Å, β = 99.25(8)°; d_{calc} = 1.19 g cm^{-3}, V = 2402.6(1) Å^3, Z = 4; μ(Mo Kα) = 7.61 cm^{-1}, range for data collection, $2\theta_{max}$ = 27.44°; ω scan; index ranges, $-16 \le h \le 16$, $0 \le k \le 22$, $0 \le l \le 17$; reflections collected 9212; independent reflections, 8055; parameters, 226; empirical absorption correction (minimum 0.846, maximum 1.194), structure solution, heavy-atom method; structure refinement, full-matrix least-squares on F; R = 0.059, R_w = 0.062 based on 5041 reflections with $I > 2\sigma(I)$. (d) **Single-crystal X-ray analysis of 7**:[9e] size, 0.25 × 0.36 × 0.43 mm, Enraf-Nonius CAD4 diffractometer; Mo Kα (graphite monochromator, λ = 0.710 69 Å), empirical formula, $C_{23}H_{46}P_2Fe$, space group, $P\bar{1}$; unit cell dimensions, a = 9.719(2) Å, b = 13.667(3) Å, c = 18.787(1) Å, α = 83.516(9)°, β = 83.513(8)°, γ = 87.53(2)°; d_{calc} = 1.19 g cm^{-3}, V = 2462.5(1) Å^3, Z = 4; μ(Mo Kα) = 7.44 cm^{-1}, range for data collection, $2\theta_{max}$ = 27.44°; ω scan; index ranges, $-13 \le h \le 13$, $-18 \le k \le 18$, $0 \le l \le 25$; reflections collected, 11 108; independent reflections, 11 108; parameters, 469; no absorption correction; structure solution, heavy-atom method; structure refinement, full-matrix least-squares on F; R = 0.044, R_w = 0.050 based on 7041 reflections with $I > 2\sigma(I)$. (e) Atomic coordinates and esd's have been deposited at the Cambridge Crystallographic Data Centre.

(10) (a) Hoberg, H.; Jenni, K.; Krüger, C. *Angew. Chem.* **1987**, *99*, 141. (b) Jenni, K. Doctoral Dissertation; Universität Bochum, 1987.

(11) Doman, T. N.; Landis, C. R.; Bosnich, B. *J. Am. Chem. Soc.* **1992**, *114*, 7264.

(12) Bosnich, B. *Chem. Soc. Rev.* **1994**, 387.

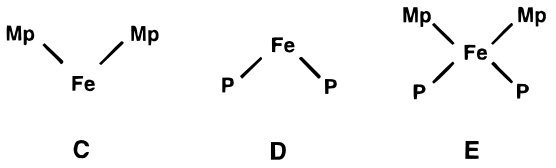

Figure 1. Molecular fragments to be fitted for the comparison of different parameter sets.

constants for the valence angles at the metal atom this should allow for a range of Fe(bis-phosphine) species having widely varying P−Fe−P angles to be tested.

The force constants of the potential functions for the coordination geometry of the iron atom (Table 1) have been manually optimized using the Box-Wilson-method[13] as initially applied by Lutz.[5a] This statistical approach enables the effect of individual parameters upon the whole to be assessed with a minimum of variations. The crystal structures of **4a**, **5**, and **6**, which served as a test set, have been fully optimized using the different parameter sets. On the basis of the measure of agreement (root-mean-square (*rms*) deviation of selected fragments; see Figure 1) between the crystal structures and the calculated structures, the quality of the parameter sets has been determined.

A comparison of the structures calculated using the optimized parameters and the reference structures is shown in Figure 2 along with the crystal structures and calculated structures of the principal isomer of **4** (**4b**, *cisoid* hexadiene), (η^2:η^2-1,5-C_6H_{10})Fe(PEt_3)$_2$ (**8a**),[2] and (η^2:η^2-1,6-C_7H_{12})Fe($Pr^i_2PC_3H_6PPr^i_2$) (**9a**).[2]

The TMS deviation of the best fit between the orthogonal coordinates for calculated structure and crystal structure based upon the partial structures **C**−**E** (Figure 1) are listed in Table 2 along with those for all atoms other than hydrogen. The comparison shows that the ($R_2P(CH_2)_nPR_2$)Fe fragment is reproduced accurately for all structures. This important point is mainly the result of the optimization of the phosphine parameters which had been carried out previously[5−8] and only needed adjustment for the parameters specific to iron. The reproduction of the organic ligands is good for the diastereomeric forms of the hexadiene complexes **4** and the cyclooctadiene complex **5**. Furthermore, the calculations show that the two diastereomeric forms of the 1,5-hexadiene complex **4** (*cisoid* and *transoid*) differ by only 0.03 kcal/mol and, hence, it is not surprising that both forms are present in the crystal. However, the ethylene ligands in **6** and **7** and the 1,6-heptadiene ligand in **9** are not satisfactorily reproduced. This reflects the difficulty in extending the results for systems containing the relatively strained hexadiene and cyclooctadiene groups to systems containing the strain-free groups ethylene and heptadiene. The discrepancies in the torsion angles between the calculated structure and crystal structure are particularly large for **9**: the double bonds and the metal atom are almost in the same plane, with the heptadiene molecule adopting an energetically favorable chair conformation. If we bear in mind that changes in the torsion angle do not in general have a large influence on the total energy of the system, it is possible that a favorable arrangement in the crystal can more than compensate for any effects

(13) Box, G. E. P.; Wilson, K. B. *J. R. Stat. Soc.* **1951**, *B13*, 1.

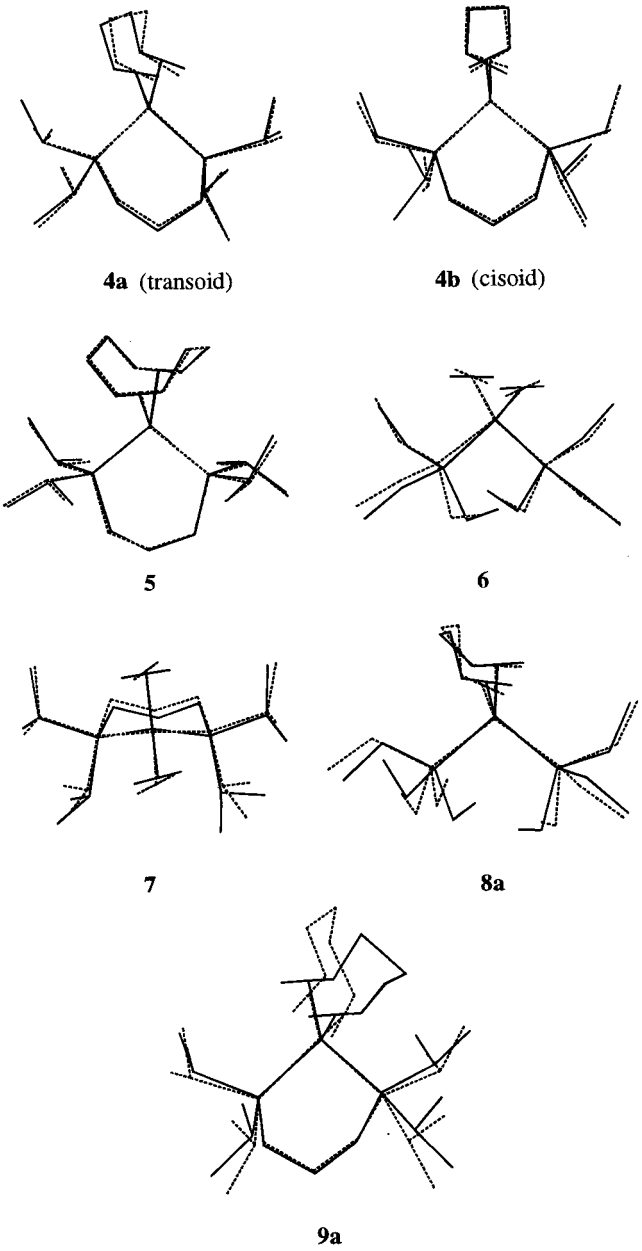

Figure 2. Superimposition of the crystal structures (dotted lines) and modeled structures (solid lines). Only the major isomer of **9** (**9a**, *transoid* diene) is shown.

Table 2. Comparison of the Calculated Structure and Crystal Structure for the Compounds Shown in Figure 2 Based on the rms Deviation from the Orthogonal Atomic Coordinates of the Three Partial Structures C−E and for All Atoms Other than Hydrogen

	rms value (Å)			
	partial structure			all atoms except H atoms
compd	C	D	E	
4a	0.0246	0.0060	0.0932	0.1793
4b	0.0086	0.0258	0.1004	0.1902
5	0.0365	0.0231	0.0536	0.1292
6	0.0063	0.0553	0.0714	0.2094
7	0.1827	0.0226	0.1927	0.3933
8a	0.0105	0.0895	0.0810	0.4644
9a	0.1606	0.0537	0.1620	0.6730

associated with changes in the torsion angles. The crystal structure of **9** shows analogies to that of the trigonal-planar (η^2:η^2-1,6-heptadiene)$NiPR_3$ complexes.[14]

Scheme 2

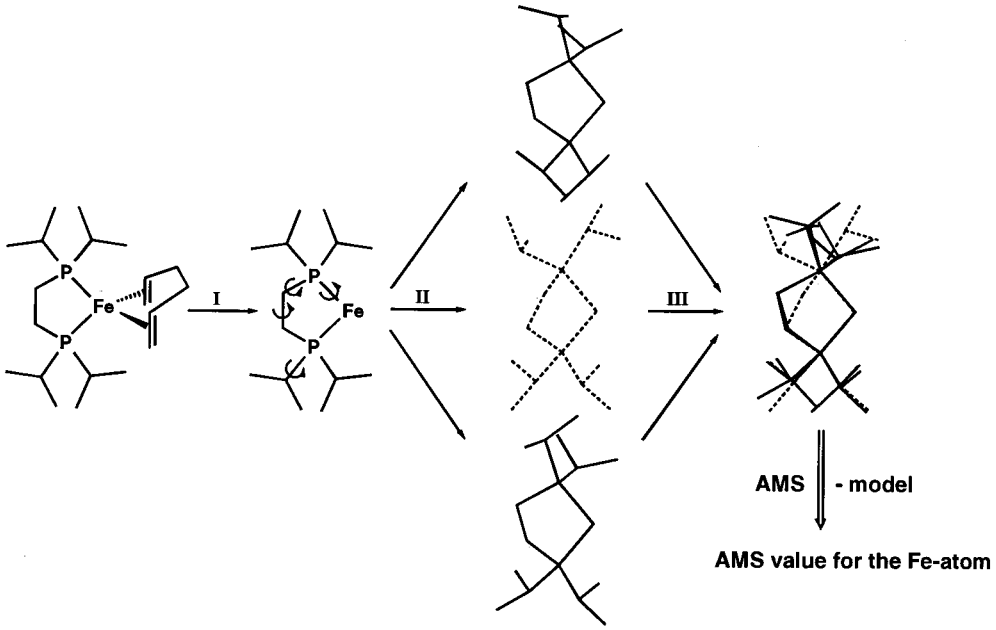

For our purposes, it is significant that the complete parameter set which we have developed for the TRIPOS force field enables us to calculate the (η^2:η^2-1,5-hexadiene)Fe($R_2P(CH_2)_nPR_2$) complexes with sufficient accuracy, and the results encourage us to subject these compounds to the molecular modeling treatment presented below.

CAMD Investigations

The (η^2:η^2-1,5-hexadiene)Fe complexes have been analyzed by means of computer-aided molecular design (CAMD). In addition to (η^2:η^2-1,5-C_6H_{10})Fe($Pr^i_2PC_3H_6PPr^i_2$) (**4**) and (η^2:η^2-1,5-C_6H_{10})Fe(PEt_3)$_2$ (**8**), for which the minimized crystal structures have been derived (see above), we have used the valence force field to generate a series of model compounds of the type (η^2:η^2-1,5-C_6H_{10})Fe($R_2P(CH_2)_nPR_2$) where R = Pr^i and n = 1, 2, 4, and 5 and where R = cyclopentyl (cyp), cyclohexyl (cyh), and *tert*-butyl and n = 2.

With energy-minimized structures as a starting point, the conformational space of these complexes was probed (Scheme 2, path I) as described in more detail in the Experimental Section. Conformations of low energy (Scheme 2, path II) were selected and subsequently superimposed in such a way to best fit the FeP_2 fragment (Scheme 2, path III). The results for a series of ($Pr^i_2P(CH_2)_nPPr^i_2$)Fe^0-fragments are shown pictorially in Figure 3, which convincingly demonstrates that, for this system, the availability of the iron atom is directly related to the length of the methylene chain joining the two P atoms.

To put these results on a more quantitative basis, we have made use of the accessible molecular surface (AMS) approach.[15] In our application the AMS represents the accessible surface of the Fe atom in the molecular systems constructed as shown in Scheme 2, (path III). In a manner similar to the original Connolly program,[16] we used a probe radius of 1.4 Å (approximately the radius of a water molecule) to determine the size and shape of the AMS.

Table 3. Size of the Accessible Molecular Surface (AMS) at the Fe Atom for a Series of ($R_2P(CH_2)_nPR_2$)Fe^0 Fragments

bis-phosphine−iron fragment	product of the reaction with 1,5-hexadiene[a]	AMS (Å^2)
($Pr^i_2PCH_2PPr^i_2$)Fe	decomposition	16.7
($Pr^i_2PC_2H_4PPr^i_2$)Fe	**3**	13.8
($Cyp_2PC_2H_4PCyp_2$)Fe	**3**	12.9
($Cyh_2PC_2H_4PCyh_2$)Fe	**3** (**1**)	11.9
($Pr^i_2PC_3H_6PPr^i_2$)Fe	**1**	12.8
(Et_3P)$_2$Fe	**1**	12.1
($Pr^i_2PC_4H_8PPr^ir_2$)Fe	**1**	9.7
($Bu^t_2PC_2H_4PBu^t_2$)Fe	**1**	13.7
($Pr^i_2PC_5H_{10}PPr^i_2$)Fe	**1** (?)	5.2

[a] **3** = (η^5-1-MeC_5H_6)FeH complex; **1** = (η^2:η^2-1,5-hexadiene)Fe complex.

The results shown in Table 3 along with the products of their reaction with 1,5-hexadiene confirm the original speculation that there is indeed a correlation between the probability of further reaction with H transfer to the Fe atoms and the size of the surface area accessible to the metal center. This is gratifying but, in view of the crudeness of the approach, also somewhat surprising: among others thing, changes in bond distances and valence angles as well as electrostatic and solvent effects have not been taken into account. Whereas a discussion of the different sizes of the AMS is considered to be sufficient to clarify the topic discussed in this paper, the AMS approach could readily be further improved to include charge- and shape-related effects.

For example, in the presence of ($Pr^i_2PC_3H_6PPr^i_2$)Fe (AMS = 12.8 Å^2), the reaction terminates with formation of the η^2:η^2-1,5-hexadiene complex, whereas for ($Pr^i_2PC_2H_4PPr^i_2$)Fe (AMS = 13.8 Å^2), the metal is more

(14) Proft, B.; Pörschke, K. R.; Lutz, F.; Krüger, C. *Chem. Ber.* **1991**, *124*, 2667.

(15) (a) Angermund, K.; Baumann, W.; Dinjus, E.; Fornika, R.; Görls, H.; Kessler, M.; Krüger, C.; Leitner, W.; Lutz, F. *Chem. Eur. J.* **1997**, 3, 755. (b) Angermund, K.; Kessler, M.; Krüger, C.; Lutz, F. Manuscript in preparation.

(16) (a) Connolly, M. L. *J. Appl. Crystallogr.* **1983**, *16*, 548. (b) Connolly, M. L. *Science* **1983**, *221*, 709.

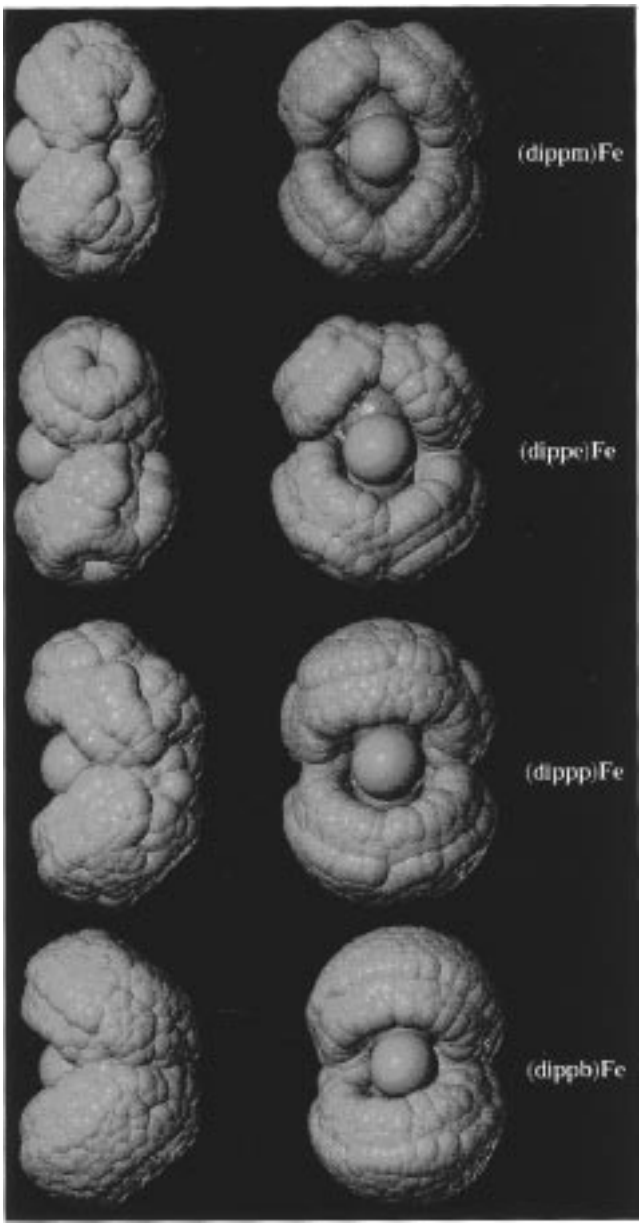

Figure 3. Pictorial representation of the overlap of selected conformations for the $(Pr^i_2P(CH)_nPPr^i_2)Fe$ fragments (dippm, $n = 1$; dippe, $n = 2$; dipp, $n = 3$; dippb, $n = 4$): violet = Fe, orange = P, turquoise = C/H.

exposed and further reaction with H transfer can occur. Significantly larger exposure of the Fe atom, e.g. $(Pr^i_2PCH_2PPr^i_2)Fe$ (AMS = 16.7 Å^2), results in further reaction and decomposition while significantly smaller exposure, e.g. $(Pr^i_2PC_5H_{10}PPr^i_2)Fe$ (AMS = 5.2 Å^2), results in encapsulation of the metal atom and the metal-diene bond is weakened.

One anomaly in the results shown in Table 3 should be mentioned: although the $(Bu^t_2PC_2H_4PBu^t_2)Fe$ fragment has the large AMS value of 13.7 Å^2, the product of the reaction with 1,5-hexadiene is the L_2Fe(diene) species and not an iron-hydride. It is conceivable that this observation is associated with restricted mutual-rotation of the sterically demanding, P-bonded *tert*-butyl groups, which as a result have less influence on the free surface area than expected.

Conclusions

The CAMD investigations presented demonstrate convincingly that for the (bis-phosphine)Fe(1,5-hexadiene) systems there is a correlation between H transfer from the coordinated diene to the metal atom and the surface area available at the metal as measured by the AMS method—the greater the surface available, the easier the hydrogen transfer. The results do, however, have a wider significance and should be applicable to other reactions involving L_2Fe^0 species and to P-donor ligands other than those described here.

Experimental Section

Computer: Silicon Graphics workstations of the types IRIS/80GTB, INDIGO2, and POWER INDIGO2.

Force Field: SYBYL[3] valence force field version 6.2/6.3, original parameter set extended by the newly developed iron parameters as described in this publication.

Energy Minimization:[17] Final minimization algorithm BFGS; recalculation of the nonbonding interactions every 10 cycles, convergence criterion TMS gradient <0.01 kcal mol^{-1}, nonbonded cutoff radius 8 Å.

Conformational Analyses: Systematic search, torsion angle increment 5° (in ring formed by Fe-atom and 1,5-hexadiene), 10° (in chelating bis-phosphine), and 30° (in P-bonded alkyl groups), ring closure bond, distance variation 0.1 Å, angle variation 5°.

Accessible Molecular Surface (AMS) of the Fe Atom: point density 50 points/Å^2, generation neighbor distances 2.0 Å, triangulation neighbor distance 1.6 Å, minimum neighbor angle 110°, maximum dot vertexes 11, probe radius 1.4 Å.

Acknowledgment. We thank Prof. K. Jonas and Dr. A. J. Frings for supplying the crystallographical data for **5** and **7**.

OM971110Q

(17) The value 0.01 kcal/mol as the final maximum derivative limit was chosen instead of 0.001 kcal/mol to avoid unnecessarily lengthy calculations. Since our interest is in exploring the conformational space of the Fe complexes, the resulting minimized structures served only as a starting point for the conformational search procedures. A test with one candidate showed no significant differences starting from a structure which has been minimized to a gradient <0.001 kcal/mol.